Climate sensitivity & resistance since the Industrial Revolution

Francisco M. Calafat[1*] & B. B. Cael[2*]

1. National Oceanography Centre, Liverpool, UK. 2. National Oceanography Centre, Southampton, UK.

*francisco.calafat@noc.ac.uk & cael@noc.ac.uk.

This paper is a non-peer reviewed preprint submitted to EarthArXiv. This paper has been submitted to *Nature Climate Change*.

Author Contributions: Calafat and Cael designed the study and performed the analysis with input from Cael. Cael and Calafat wrote the paper.

Article Type: Brief Communication

Keywords: Climate change | Bayesian statistics | Climate feedback | Pattern effect | Energy balance model | Climate sensitivity

Data Availability: Data are available from the sources cited in the text. Code will be made available at a github repository and given a DOI via Zenodo should this manuscript be accepted for publication.

Conflicts: The authors have no competing interests to declare.

Abstract: Climate sensitivity is a fundamental yet uncertain metric of Earth's response to anthropogenic forcing; its temporal evolution in particular is poorly constrained yet critical for leveraging historical observations for future projections. A Bayesian energy balance model indicates a 83% (84%) probability that the climate sensitivity increased (decreased) from 1900-1940 (1940-2010). These trends are attributable to spatial warming patterns likely to reverse in the future, and are distinct from Earth-system-model-derived analogs.

A fundamental question for international efforts to limit global warming is how sensitive Earth's climate is to radiative forcing (F, [W m^{-2} K^{-1}]) resulting from human activities. From physics to economics, an energy balance model (EBM) framework has been widely adopted to understand, quantify, and model this sensitivity, with (a) differential equation(s) similar to

$$c\frac{d\Delta T}{dt} = F - \rho\Delta T \tag{1}$$

where ΔT [K] is the global average temperature anomaly of the Earth's surface relative to a preindustrial baseline, c [J/m^2 K] is the heat capacity of the surface layer represented by ΔT, and ρ [W m^{-2} K^{-1}] is the 'climate resistance' [1].[2] The sensitivity is then most realistically quantified by the transient climate response (TCR, [K]), the estimated value of ΔT after 70 years of compounding 1% increases in atmospheric CO_2 concentrations, after which time atmospheric CO_2 has doubled.[3] Unfortunately, despite tremendous observational, theoretical, and computational efforts, the TCR and ρ are highly uncertain; providing best estimates and reducing uncertainties in these quantities are central goals of modern climate science, with societal value in the trillions of dollars [4].

These efforts have lead to improved estimates of ΔT and F over the historical period (i.e. since the Industrial Revolution, 1850-2020), which along with paleorecords of Earth's past and theoretical and computational modelling are key tools for constraining climate metrics such as ρ and TCR [5]. However, these historical observations are still surrounded by significant uncertainty.[6] A globally averaged perspective also masks important spatial differences such as the 'pattern effect' whereby warming in recent decades has been more focused in regions of tropical convection where warming is more efficient at countering radiative forcing [7].

Climate metrics like ρ and TCR are frequently estimated as time-invariant quantities. However, there is good reason to suspect that they have varied in the past 170 years, due to changes in ocean circulation and heat uptake, sea ice and vegetation cover, or changing atmospheric composition or dynamics. If ρ and TCR have changed over the historical period, this has important implications for future projections, both because it affects how historical observations are used to constrain these parameters and because it demonstrates that these quantities are liable to change in the future on multidecadal/centennial timescales. Time series of components of ρ have been diagnosed from models [8, 9], and to some extent from observations, but focusing on estimating time-invariant quantities either with increasing information over time [10] or deconvolving the effect of processes occurring with distinct timescales [11]. The temporal evolution of

ρ in historical observations has not been investigated, in particular with the full time series of historical observations and suitable statistical methods to quantify uncertainty robustly and leverage a priori information. Here we show from global F and ΔT records alone that it is likely ($\geq$83% probability) that ρ (TCR) decreased (increased) from 1900-1940 and then increased (decreased) from 1940-2010.

We make probabilistic estimates of the time evolution of ρ and its associated TCR by analyzing state-of-the-art time series of ΔT [12] and F [13, 14] for the period 1850-2020 using an EBM (Methods). We adopt a Bayesian approach, meaning that we use probability distributions to describe uncertainty in all model quantities, i.e., observational data, F, and unknown parameters. We model ΔT as the superposition of a temporal process that evolves under the influence of F plus a first-order autoregressive (AR1) process that captures the effect of internal climate variability. Observations of ΔT are modelled as noisy measurements of the true latent process ΔT, whereas F is assumed to follow a temporal Gaussian process with mean and covariance matrix extracted from an ensemble of radiative forcing time series [13, 14]. The influence of the El Niño Southern Oscillation (ENSO) is explicitly accounted for by assimilation of an observation-based ENSO index [15]. We model ρ as a time-varying parameter that evolves according to a random walk, allowing us to quantify changes in climate sensitivity through time. Our Bayesian approach has numerous advantages over traditional statistical approaches, the most important of which are: 1) it involves rigorous uncertainty quantification, accounting for uncertainty not only in observations, but also in radiative forcing, processes and parameters; 2) it allows us to incorporate prior knowledge into our analysis in a probabilistically consistent way, leading to more robust inferences. Such prior knowledge includes information about the range of plausible values for some of the model parameters, such as ρ and the heat capacity of the surface layer (dominated by the ocean mixed layer); and 3) it enables us to make direct probability statements relevant to the questions of interest, such as whether the TCR in one year is different form that in another year. Before discussing our results, we note that our results are robust to a number of adjustments to priors and model formulation (Methods), and that the evolution of climate feedback λ and ocean heat uptake efficiency κ could be separated using an ocean heat uptake time series, but would be sensitive to the substantial differences between different observational reconstructions [16, 17] and that for transient climate behaviour relevant to economic modelling and policy, the climate resistance ρ is arguably the more relevant parameter.

Separating forced changes in ΔT from internal climate variability and noise shows unambiguously that global average surface temperature has been accelerating since 1850 (Fig. 1a), with an initial period of slow or no change from 1850 to 1915, followed by a period of rapid warming with an increased rate of temperature rise since 1970. Superimposed on these long-term changes, there are marked short-term dips in ΔT caused by the cooling effect of aerosols emitted by volcanic eruptions (Extended Data Fig. 1), the most prominent ones occurring three years after the eruptions of Krakatoa (1883), Agung (1963), and Pinatubo (1991). Focusing on ρ, the Bayesian solution shows a significant multidecadal fluctuation (Fig. 1b), starting with a value of 2.22$\pm$0.37 W m^{-2} K^{-1} ($\pm$1 posterior s.d.) in 1850 that gradually increases to 2.35$\pm$0.50 W m^{-2} K^{-1} by 1900, falling then rapidly to a value of 1.95$\pm$0.45 W m^{-2} K^{-1} in 1940, and finally bouncing back to a value of 2.33$\pm$0.25 W m^{-2} K^{-1} in 2010. The time-mean value of ρ is estimated to

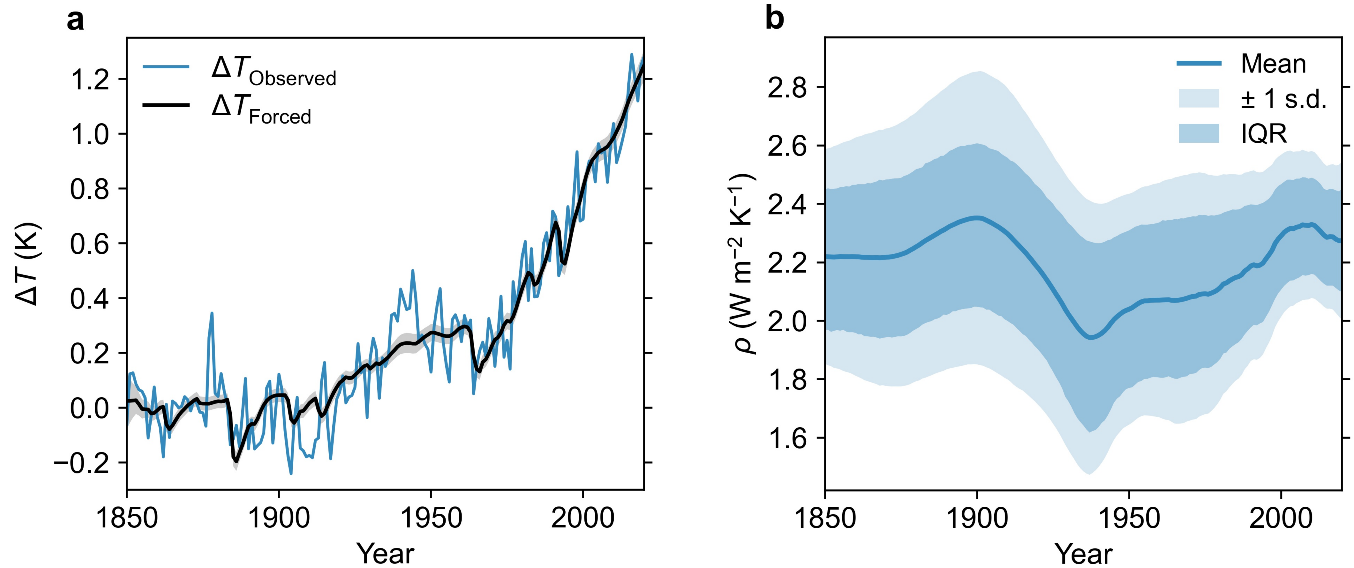

Figure 1: a) Observed global mean surface temperature anomaly from HadCRUT5 [12] (blue) and the same after internal climate variability (ENSO influence plus an AR1 process) and white noise have been removed (posterior mean in black, with grey shading representing one standard deviation uncertainty). b) Climate resistance versus time; blue line represents the posterior mean while the light and dark blue shading represent one standard deviation uncertainty and the interquartile range (IQR), respectively.

be 2.19±0.33 W m^{-2} K^{-1}, consistent with past observational estimates [10].[18] Credible intervals for the time series of ρ show a tendency to become narrower over the historical period as uncertainty in the ΔT observations decreases, and F and the rate of warming increase. While the uncertainty associated with estimates of ρ is large relative to the magnitude of the temporal changes, we nonetheless find it likely (probability $P = 0.83$ and 0.84) that the values of ρ in 1900 and 2010 are larger than the value in 1940 (Fig. 2a). Lower values of ρ imply a stronger temperature response to radiative forcing and vice versa. Hence the temporal changes in ρ discussed above indicate that the rate of temperature change per unit radiative forcing is not constant with time but it varies noticeably on multidecadal time scales. We note that this general temporal pattern is qualitatively similar to that the model-based time series of the climate feedback found in [8], though the magnitude of the variations is much smaller, and has periods of both qualitative similarity and disagreement with those in [9, 11, 10]. Depending on the study in question, these discrepancies may be methodological, due to changes in ocean heat uptake efficiency, or between historical observations and simulations of climate. Regardless, as none of these studies were explicitly designed to estimate the time-evolution of ρ from observations, our study serves as a useful benchmark for comparison or model evaluation and supports that model-derived temporal changes in climate feedback are not model artefacts.

These multidecadal changes in ρ correspond to substantial changes in the TCR (Fig. 2b). TCR shifts from 1.69±0.38 in 1900 to 2.03±0.55 in 1940, then back to 1.65±0.21 in 2010, implying changes over time of 0.3-0.4 K. This last estimate is slightly higher than the value of 1.5 K (5-95% range 1.3-1.8) from [19] and on the lower end of the 66% range of 1.5-2.2 K from [5]; all estimates are within the very wide IPCC AR5 range of 1.0-2.5 K. Note that a TCR of 2.01 K versus a TCR of 1.64 implies another 15 years of compounded increases in atmospheric CO_2 concentrations before ΔT

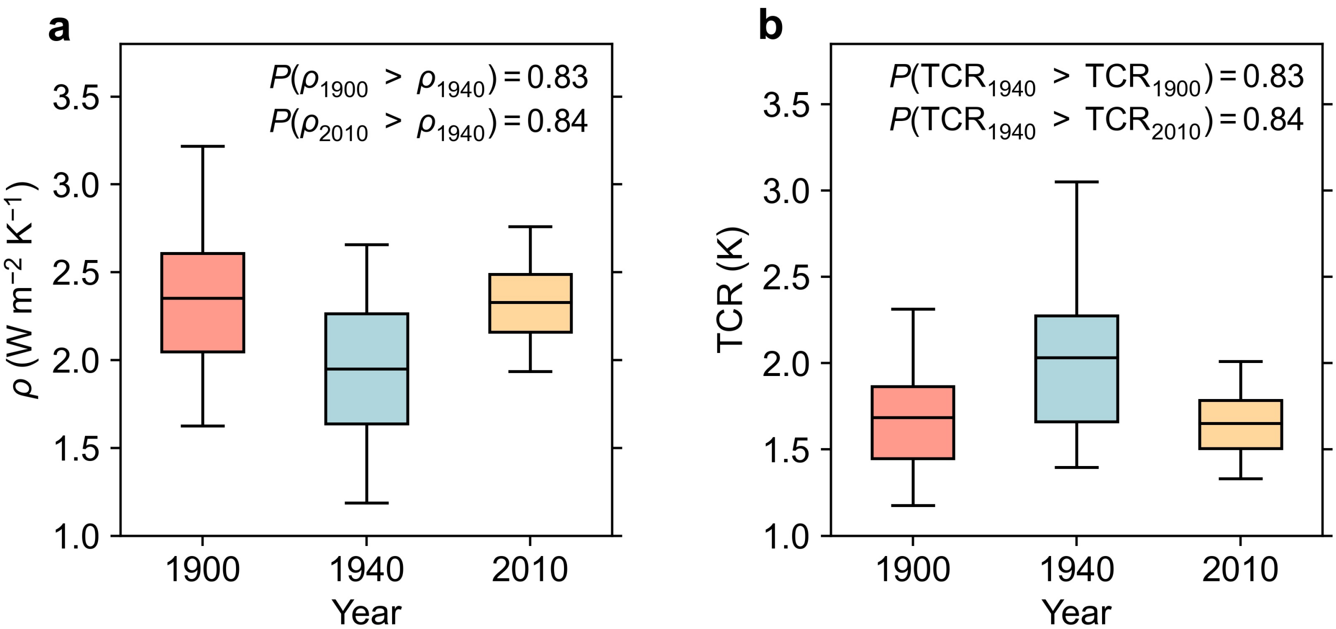

]

Figure 2: Box-and-whisker plots showing the posterior mean (central mark), interquartile range (shaded box), and 5-95% credible interval (whiskers) for the climate resistance (a) and associated transient climate response (b) for the years with local extrema in the posterior mean in Figure 1b. Posterior probabilities that the climate resistance (or transient climate response) is smaller (larger) in 1940 than 1900 or 2010 are given in the top-right corner of each panel.

reaches two degrees.

Altogether our results suggest that ρ and TCR have likely shifted by about 0.3-0.4 W/m^{2}K and K respectively ($\geq$83% probability) over 1900-1940 and 1940-2010. Such multidecadal shifts in these core climate metrics must be accounted for when leveraging historical observations to make future projections, including the propensity of such parameters to change in the future. The cause of these variations cannot be inferred from Bayesian outputs alone, but it is likely related to the dependence of ρ, and thus ΔT, on the spatial pattern of warming – the so-called pattern effect [7] – as periods of lower ρ correspond to periods when relatively more warming occurred in higher latitudes. This implies that the trend in ρ (and equivalently TCR) will reverse in the near future, as may already be the case since 2010 (Fig. 2a), as warming outside of regions of tropical convection catches up with warming in tropical convection regions. What is surprising about Fig. 2a is that the effect of the pattern effect on global climate can be diagnosed from global time-series of ΔT and F alone.

Online Methods

Annual global average surface temperature anomalies spanning the period 1850-2020 and associated uncertainties are from the HadCRUT5 data set (version .5.0.1.0) of the Met Office Hadley Centre/Climatic Research Unit [12], available at https://www.metoffice.gov.uk/hadobs/hadcrut5/. The data are from the HadCRUT5 analysis which uses a statistical infilling method to extend estimates of temperature anomalies into data sparse regions, leading to more robust estimates of global average temperature changes. The time series of the ENSO index spanning the period 1850-

2020 is from the Ensemble Oceanic Niño Index [15], which are also provided with uncertainty estimates. The ensemble of radiative forcing time series is from [13].

Our goal here is to make inferences about TCR from global average surface temperature observations using a probabilistic framework that allows us to account for uncertainty in the observations, radiative forcing, and model parameters. We model the latent process ΔT as the sum of a term that represents the response to radiative forcing (ΔT_{F}) plus a term that captures the influence of internal climate variability (ΔT_{I}). We assume that the evolution of ΔT_{F} is governed by a linear zero-dimensional EBM driven by radiative forcing analogous to that described by equation (1):

$$c\frac{d\Delta T_{\mathrm{F}}(t)}{dt} = F(t) - \rho(t)\Delta T_{\mathrm{F}}(t) \tag{2}$$

in which $F(t)$ and $\rho(t)$ are, respectively, the radiative forcing and the climate resistance at time t.

In designing the model, it is important to recognize that the temperature observations are subject to significant uncertainty (arising from measurement error, spatial interpolation, etc.), and thus they only provide a noisy view of the true latent process ΔT. Furthermore, neither the radiative forcing F nor the latent processes $\rho(t)$ and ΔT_{I} are known precisely, which introduces further uncertainty into the model. Additional uncertainty enters the model through unknown model parameters, including c and other parameters that are needed to specify the latent processes such as error variances and autocorrelation coefficients. Accounting for all these sources of uncertainty is crucial to obtaining reliable estimates of TCR and realistic uncertainty intervals. Here, we achieve this by specifying a dynamic model as a Bayesian hierarchical model with three levels: 1) a probability model that describes the distribution of the temperature observations and the ENSO index reanalysis conditional on the true latent processes (data model); 2) a probability model that describes the dynamics of the latent processes conditional on a set of parameters (process model); and 3) a prior distribution that describes the uncertainty in the model parameters and encodes our prior knowledge about the data and the processes (parameter model). Inferences from our model are made by evaluating the posterior distribution of the processes and parameters given the observations, which is proportional to the product of the three probability models that form the hierarchy. In the following, we describe the three levels of the hierarchical model.

Let y_t denote the global surface temperature observation at year t. Then, by discretizing in time, the data model for the temperature observations can be written as:

$$y_t = \Delta T_{\mathrm{F},t} + \Delta T_{\mathrm{I},t} + m + \epsilon_{\mathrm{y},t}, \qquad t = 1, ..., T \tag{3}$$

Where m is an unknown offset, and $\epsilon_{\mathrm{y},t}$ is a mean-zero Gaussian observation error with standard deviation set equal to the standard errors provided by the HadCRUT5 product, which vary from year to year with larger errors at the beginning of the record. Note that we assume independence of observation errors.

In addition to the temperature observations, we also use an observation-based ENSO index ($x^{\mathrm{Obs}}_{\mathrm{Enso},t}$) to explicitly capture variability in ΔT_{I} associated with ENSO. The ENSO index data are subject to uncertainty, which we account for by modelling such data as a noisy version of the true ENSO index ($x_{\mathrm{Enso},t}$):

$$x^{\mathrm{Obs}}_{\mathrm{Enso},t} = x_{\mathrm{Enso},t} + \epsilon_{\mathrm{Enso},t} \tag{4}$$

where $\epsilon_{\mathrm{Enso},t}$ is a mean-zero Gaussian data error with time-varying standard deviation set equal to the standard errors provided by the ENSO index product.

Next we describe the process level of the model. The process $\Delta T_{\mathrm{I},t}$ is split into a term that describes the influence of ENSO ($\Delta T^{\mathrm{Enso}}_{\mathrm{I},t}$) plus a residual term that captures internal variability unrelated to ENSO ($\Delta T^{\mathrm{Res}}_{\mathrm{I},t}$). With that, the process level comprises five temporal processes, namely $\Delta T_{\mathrm{F},t}$, F_t, ρ_t, $\Delta T^{\mathrm{Enso}}_{\mathrm{I},t}$ and $\Delta T^{\mathrm{Res}}_{\mathrm{I},t}$. As mentioned above, $\Delta T_{\mathrm{F},t}$ is assumed to follow Equation (2).

The radiative forcing F_t is modelled as:

$$F_t \sim N(\mu_{\mathrm{F},t}, \Sigma_{\mathrm{F}}) \tag{5}$$

where $\mu_{\mathrm{F},t}$ and Σ_{F} are, respectively, the mean and the temporal covariance matrix extracted from the ensemble of radiative forcing time series.

The climate resistance parameter ρ_t is assumed to follow a random walk:

$$\rho_t = \rho_{t-1} + \epsilon_{\rho,t} \tag{6}$$

where $\epsilon_{\rho,t}$ is Gaussian white noise with unknown standard deviation σ_{ρ}. The initial value of the climate resistance parameter ($\rho_0 := \rho_{t=0}$) is unknown and is modelled in the parameter layer of the hierarchical model by placing a prior distribution on it.

The ENSO index is assumed to follow a zero-mean AR1 process:

$$x_{\mathrm{Enso},t} = \phi_{\mathrm{Enso}} x_{\mathrm{Enso},t-1} + \epsilon_{\mathrm{Enso},t} \tag{7}$$

in which ϕ_{Enso} is the AR1 autocorrelation coefficient for the ENSO index process, and $\epsilon_{\mathrm{Enso},t}$ is Gaussian white noise with unknown standard deviation σ_{Enso}. The initial value $x_{\mathrm{Enso},0} := x_{\mathrm{Enso},t=0}$ is modelled in the parameter layer. Then, the effect of ENSO on ΔT is given by the linear regression:

$$\Delta T_{\mathrm{I},t}^{\mathrm{Enso}} = \beta x_{\mathrm{Enso},t} \tag{8}$$

where β is the regression coefficient associated with $x_{\mathrm{Enso},t}$.

Finally, the process $\Delta T_{\mathrm{I},t}^{\mathrm{Res}}$ is modelled as an AR1 process:

$$\Delta T_{\mathrm{I},t}^{\mathrm{Res}} = \phi_{\mathrm{Res}} \Delta T_{\mathrm{I},t-1}^{\mathrm{Res}} + \epsilon_{\mathrm{I},t} \tag{9}$$

where ϕ_{Res} is the AR1 autocorrelation coefficient, and $\epsilon_{\mathrm{I},t}$ is Gaussian white noise with unknown standard deviation σ_{I}. The initial value $\Delta T_{\mathrm{I},0}^{\mathrm{Res}} := \Delta T_{\mathrm{I},t=0}^{\mathrm{Res}}$ is modelled in the parameter layer.

The total contribution from internal climate variability is: $\Delta T_{\mathrm{I},t} = \Delta T_{\mathrm{I},t}^{\mathrm{Enso}} + \Delta T_{\mathrm{I},t}^{\mathrm{Res}}$.

The parameter level is summarized in Extended Data Table 1. Next, we provide justification for some of the more informative priors. ρ_0 is given a log-normal prior of $lnN(0.8, 0.2)$. The choice of a log-normal parameterisation is because the log-normal distribution is its own inverse distribution, so choosing a log-normal prior for ρ yields a log-normal prior for any climate sensitivity metric $S \propto \rho^{-1}$, and vice versa; this therefore avoids some of the issues with implausibly heavy tails that arise in priors for S (ρ) when choosing a prior for ρ (S) [5]. The choice of parameter values is based on the sum of the surface layer's constrained energy balance responses (Planck feedback, surface albedo feedback, water vapor lapse rate feedback, and energy flux into ocean interior) with values taken from [5] and uncertainty estimates combined in quadrature; the corresponding Gaussian distribution is replaced by the log-normal distribution with the same mean and standard deviation. c is given a Gaussian prior $N(9.67, 0.8)$ which is calculated from the number of seconds in a year (to make the HadCRUT5 timestep comparable to the units of the radiative forcing time series), the mean mixed layer depth (equally weighted in area and time) of the Argo mixed layer climatology [20], the density and heat capacity of seawater, and the sea surface temperature to global mean surface temperature warming ratio of HadSST4 [21] and HadCRUT5 [12]. We note that this prior is in good agreement with the c values estimated for the CMIP5 ensemble in [22] and that the uncertainty is dominated by uncertainty in which method is used to define the mixed layer depth.

The Bayesian hierarchical model is fitted using the No-U-Turn Sampler (NUTS) as implemented by the Stan probabilistic programming language [23]. We run the sampler with four chains of 3500 iterations each (warm-up=1000) for a total of 10000 post-warm-up draws. Our fits did not show any divergent transitions and none of the iterations saturated the maximum tree depth, indicating that the sampler is able to explore the posterior distribution adequately. Convergence and mixing diagnostics for the model parameters are provided in Extended Data Table 1.

The TCR is not a direct output of the Bayesian model, but it can be calculated as follows. First, at each iteration of the NUTS sampler and for each year (1850-2020), we generate a 70-year time series of radiative forcing linearly increasing from 0 to a value, ΔF_{2xCO_2}, that corresponds to a CO_2 doubling. Following [5], ΔF_{2xCO_2} is drawn from a normal distribution $\Delta F_{2xCO_2} \sim N(4.0, 0.3)$. This time series is then used to force the EBM as defined by Equation (1), in which the values of c and ρ are set equal to the Bayesian estimates at the corresponding sampler iteration and year. Solving Equation (1) then yields a 70-year time series of changes in temperature, and the TCR is taken to be the temperature change at year 70. This procedure gives estimates of TCR in the form of samples from the posterior distribution. We also note that this provides very similar results to a simpler TCR $= 4/\rho$ [10] but is more in keeping with the standard definition of TCR.

To assess the sensitivity of our results to prior choices, we compare estimates of ρ and the TCR based on different priors for σ_ρ and ρ_0. These two parameters control the properties of the random walk that governs the evolution of ρ and, thus, they have the largest influence on both ρ and the TCR. The actual priors that we use for σ_ρ and ρ_0 in this study are half$N(0, 0.1)$ and $lnN(0.8, 0.2)$, respectively. Estimates based on these priors are compared to those based on the following much more diffuse priors: half$N(0, 0.3)$ and $lnN(0.8, 0.5)$. The results of this sensitivity experiment are summarized in Extended Data Table 2. The Bayesian estimates for all the analysed quantities are highly consistent between the two sets of priors, with differences in the posterior means that are significantly smaller than the corresponding posterior standard deviations in all cases. These results indicate that the observations are sufficiently informative to constrain the evolution of ρ, and thus the TCR, through time. We note that the noise shock parameter σ_ρ's posterior is confined to relatively small values irrespective of the prior we use. This indicates that the smaller variations in ρ over time that we find, as compared to model-based results from regressions on 30-year moving windows such as in [8], is not an artefact of our method. We also note, that the posterior standard deviations tend to be larger when using the more diffuse priors, especially for estimates prior to 1950 (e.g., ρ_{1900}). This suggests that the large observation errors in the first part of the historical record lead to relatively weak identification of the likelihood, allowing the diffuse priors to pull the posterior towards larger values. In this case, it is important to incorporate prior information into the Bayesian model through priors in order to regularize the posterior and ensure more robust inferences. This is the reason for choosing the more informative set of priors. Note that a half$N(0, 0.3)$ prior on σ_ρ means that we expect ρ to change by as much as 0.3 W K^{-1} m^{-2} between consecutive years (or by 51 W K^{-1} m^{-2} over the period 1850-2020), which conflicts with basic physical expectation. Similarly, a $lnN(0.8, 0.2)$ prior on ρ_0 means that we expect values of ρ as small as 1 or as large as 5 W K^{-1} m^{-2} to be probable (these values correspond to the 5th and 95th percentiles for this prior), which again is contrary to our expectations. We also tested a formulation of the model that used multiplicative rather than additive random walk noise shocks, and one using a random walk in sensitivity ($1/\rho$) rather than resistance, and found that these gave similar results.

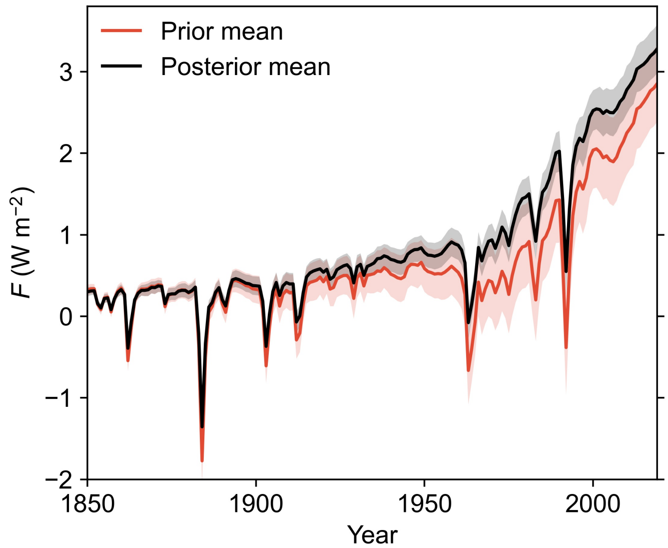

Extended Data Fig.1: Time series of prior and posterior means, with shading representing ± 1 s.d. uncertainty, of F.

Extended Data Table1. Prior distributions, parameters and convergence diagnostics. Posterior distribution mean and 5-95% credible interval for the parameters of the Bayesian hierarchical model, along with the prior distribution ascribed to each parameter. The potential scale reduction statistic (R-hat) and the effective sample size per iteration (n_{eff}/it) are also shown. In general, R-hat should be close to 1 at convergence, whereas n_{eff}/it>0.003 indicates low autocorrelation.

Parameter	Units	Description	Mean	5th	95th	Prior distribution	*R*-hat	n_{eff}/it
C	J K^{-1} m^{-2}	Heat Capacity	10.01	8.78	11.25	$\mathcal{N}(9.67,0.8)$	1.00	1.41
m	K	Constant offset	-0.11	-0.18	-0.04	$\mathcal{N}(0,0.2)$	1.00	0.62
σ_{ρ}	W K^{-1} m^{-2}	Standard deviation	0.06	0.01	0.13	half-$\mathcal{N}(0,0.1)$	1.00	0.12
ρ_0	W K^{-1} m^{-2}	Initial value	2.22	1.65	2.85	$\log\mathcal{N}(0.8,0.2)$	1.00	0.69
ϕ_{Enso}	-	AR1 Coefficient	0.21	0.09	0.34	uniform(0,1)	1.02	0.03
σ_{Enso}	K	Standard deviation	0.54	0.50	0.59	half-$\mathcal{N}(0,1)$	1.01	0.08
$x_{\mathrm{Enso},0}$	K	Initial value	-0.05	-0.84	0.77	$\mathcal{N}(0,0.5)$	1.00	1.53
β	-	Regression coefficient	0.06	0.04	0.09	$\mathcal{N}(0,1)$	1.00	0.27
ϕ_{Res}	-	AR1 Coefficient	0.42	0.24	0.58	$\mathcal{N}(0.6,0.2)$	1.00	0.17
σ_{I}	K	Standard deviation	0.08	0.07	0.09	half-$\mathcal{N}(0,0.15)$	1.00	0.31
$\Delta T_{\mathrm{I},0}^{\mathrm{Res}}$	K	Initial value	-0.05	-0.47	0.37	$\mathcal{N}(0,0.3)$	1.00	1.15

Extended Data Table 2. Sensitivity of ρ and TCR to prior distributions. Estimates (posterior mean ± 1 s.d.) of various quantities related to ρ and TCR based on different priors for σ_{ρ} and ρ_0.

Quantity	Priors on σ_ρ/ρ_0	
	half-$\mathcal{N}$(0,0.1) log$\mathcal{N}$(0.8,0.2)	half-$\mathcal{N}$(0,0.3) log$\mathcal{N}$(0.8,0.5)
σ_ρ (W K^{-1} m^{-2})	0.06±0.04	0.08±0.06
ρ_0 (W K^{-1} m^{-2})	2.22±0.36	2.18±0.68
ρ_{1900} (W K^{-1} m^{-2})	2.35±0.50	2.46±0.77
ρ_{1940} (W K^{-1} m^{-2})	1.95±0.45	1.84±0.53
ρ_{2010} (W K^{-1} m^{-2})	2.33±0.25	2.34±0.29
TCR_{1900} (K)	1.69±0.38	1.68±0.53
TCR_{1940} (K)	2.03±0.55	2.20±0.70
TCR_{2010} (K)	1.65±0.21	1.65±0.23
$P(\rho_{1900} > \rho_{1940})$	0.83	0.87
$P(\rho_{2010} > \rho_{1940})$	0.84	0.87
$P(\mathrm{TCR}_{1940} > \mathrm{TCR}_{1900})$	0.83	0.87
$P(\mathrm{TCR}_{1940} > \mathrm{TCR}_{2010})$	0.84	0.87

Acknowledgments

Calafat and Cael acknowledge NERC strategic funding through Enhancing Climate Observations, Models and Data. We thank Jonathan Gregory and Jonah Bloch-Johnson for insightful comments.

References

[1] JM Gregory and PM Forster. "Transient climate response estimated from radiative forcing and observed temperature change". *Journal of Geophysical Research: Atmospheres* 113.D23 (2008).

[2] "ρ is the sum of the upwards energy flux per unit warming λ (or α, the climate feedback), and the downwards energy flux per unit warming (κ, the ocean heat uptake efficiency), so $\rho = \lambda + \kappa$. These terms and symbols are sometimes interchanged in different publications [1, 10]." ().

[3] "The effective or equilibrium climate sensitivity are also commonly used metrics, but these are based on more idealized greenhouse gas emissions trajectories and are in any case closely related to TCR [5]." ().

[4] Chris Hope. "The \$ 10 trillion value of better information about the transient climate response". *Philosophical Transactions of the Royal Society A: Mathematical, Physical and Engineering Sciences* 373.2054 (2015), p. 20140429.

[5] SC Sherwood et al. "An assessment of Earth's climate sensitivity using multiple lines of evidence". *Reviews of Geophysics* 58.4 (2020), e2019RG000678.

[6] "n the case of ΔT there is considerable uncertainty due to measurement error and data sparseness, especially in the early part of the historical record (before 1950), whereas F exhibits persistent uncertainty arising from numerous sources (Extended Data Fig. 1) [13, 14]. Furthermore, ΔT also shows a great deal of inter-annual to multi-decadal variability associated with internal climate variability (Fig. 1a), which complicates efforts to quantify the response to radiative forcing." ().

[7] Yue Dong et al. "Attributing Historical and Future Evolution of Radiative Feedbacks to Regional Warming Patterns using a Green's Function Approach: The Preeminence of the Western Pacific". *Journal of Climate* 32.17 (2019), pp. 5471–5491. DOI: 10.1175/JCLI-D-18-0843.1. URL: https://journals.ametsoc.org/view/journals/clim/32/17/jcli-d-18-0843.1.xml.

[8] Timothy Andrews et al. "Accounting for changing temperature patterns increases historical estimates of climate sensitivity". *Geophysical Research Letters* 45.16 (2018), pp. 8490–8499.

[9] JM Gregory et al. "How accurately can the climate sensitivity to CO_2 be estimated from historical climate change?" *Climate Dynamics* 54.1 (2020), pp. 129–157.

[10] Lauren E Padilla, Geoffrey K Vallis, and Clarence W Rowley. "Probabilistic estimates of transient climate sensitivity subject to uncertainty in forcing and natural variability". *Journal of Climate* 24.21 (2011), pp. 5521–5537.

[11] Philip Goodwin. "Probabilistic projections of future warming and climate sensitivity trajectories". *Oxford Open Climate Change* 1.1 (2021), kgab007.

[12] Colin P Morice et al. "An updated assessment of near-surface temperature change from 1850: The HadCRUT5 data set". *Journal of Geophysical Research: Atmospheres* 126.3 (2021), e2019JD032361.

[13] Christopher J Smith et al. "Energy budget constraints on the time history of aerosol forcing and climate sensitivity". *Journal of Geophysical Research: Atmospheres* 126.13 (2021), e2020JD033622.

[14] V. Masson-Delmotte et al. *Climate Change 2021: The Physical Science Basis. Contribution of Working Group I to the Sixth Assessment Report of the Intergovernmental Panel on Climate Change*. 2021.

[15] Eric J Webb and Brian I Magi. "The Ensemble Oceanic Nino Index". *International Journal of Climatology* (2022).

[16] Laure Zanna et al. "Global reconstruction of historical ocean heat storage and transport". *Proceedings of the National Academy of Sciences* 116.4 (2019), pp. 1126–1131.

[17] Geoffrey Gebbie and P Huybers. "The little ice age and 20th-century deep Pacific cooling". *Science* 363.6422 (2019), pp. 70–74.

[18] "Though as previously noted our estimates span a longer time period, explicitly resolve the temporal evolution of this parameter, use improved ΔT and F data, and are derived using preferred methodology." ().

[19] Philip Goodwin and BB Cael. "Bayesian estimation of Earth's climate sensitivity and transient climate response from observational warming and heat content datasets". *Earth System Dynamics* 12.2 (2021), pp. 709–723.

[20] James Holte et al. "An Argo mixed layer climatology and database". *Geophysical Research Letters* 44.11 (2017), pp. 5618–5626.

[21] John J Kennedy et al. "An ensemble data set of sea surface temperature change from 1850: The Met Office Hadley Centre HadSST. 4.0. 0.0 data set". *Journal of Geophysical Research: Atmospheres* 124.14 (2019), pp. 7719–7763.

[22] Nicholas J Lutsko and Max Popp. "Probing the sources of uncertainty in transient warming on different timescales". *Geophysical Research Letters* 46.20 (2019), pp. 11367–11377.

[23] Bob Carpenter et al. "Stan: A probabilistic programming language". *Journal of statistical software* 76.1 (2017).